



Vaasan yliopisto
UNIVERSITY OF VAASA

OSUVA Open
Science

This is a self-archived – parallel published version of this article in the publication archive of the University of Vaasa. It might differ from the original.

Research on nitrogen reduction performance of various modes combined air-staged with air humidification for gas boiler

Author(s): Zhang, Q.; Guo, Y.; Liu, T.; Zhao, W.; Qiu, S.; Lü, X.

Title: Research on nitrogen reduction performance of various modes combined air-staged with air humidification for gas boiler

Year: 2024

Version: Accepted manuscript

Copyright ©2024 Springer. This is a post-peer-review, pre-copyedit version of an article published in *Thermophysics and Aeromechanics*. The final authenticated version is available online at:
<http://dx.doi.org/10.1134/S0869864324060258>

Please cite the original version:

Zhang, Q., Guo, Y., Liu, T., Zhao, W., Qiu, S., & Lü, X. (2024). Research on nitrogen reduction performance of various modes combined air-staged with air humidification for gas boiler. *Thermophysics and Aeromechanics* 31(6), 1349-1366.
<https://doi.org/10.1134/S0869864324060258>

Research on nitrogen reduction performance of various modes combined air-staged with air humidification for gas boiler

Q. Zhang^{1,2}, Y. Guo^{1,2}, T. Liu¹, W. Zhao¹, S. Qiu¹, and X. Lü^{1,3,4}

¹Beijing Key Lab of Heating, Gas Supply, Ventilating and Air Conditioning Engineering, Beijing University of Civil Engineering and Architecture, Beijing, China

²Collaborative Innovation Center of Energy Conservation & Emission Reduction and Sustainable Urban-Rural Development in Beijing, Beijing, China

³Department of Electrical Engineering and Energy Technology, University of Vaasa, Vaasa, Finland

⁴Department of Civil Engineering, Aalto University, Espoo, Finland

Abstract

NO_x emissions from gas boilers pose a significant threat to air quality. To significantly decrease NO_x emission level from the gas boiler exhaust, a novel nitrogen reduction combustion method is proposed that combines air-staging with humidification combustion techniques. A comprehensive study was conducted using CHEMKIN software to analyse the nitrogen reduction performance and sensitivity in various compound modes. The impact of combustion temperature, excess air coefficient, and injection position of over-fire air on the nitrogen reduction performance in the optimal compound mode was investigated. The results showed that the nitrogen reduction effect of the compound mode was better than that of the pure staged combustion mode. Compared with pure staged combustion, humidifying the main combustion zone could improve the nitrogen reduction rate by 4.9 %, which was 1.7 % higher than humidifying the burnout zone. The most significant nitrogen reduction effect was achieved when both combustion zones were humidified, leading to a 7.4 % increase in the nitrogen reduction rate. Further, by humidifying both combustion zones and reducing the combustion temperature, the emission of NO during boiler operation was found to be reduced significantly. The nitrogen reduction rate can be increased to 65.7 %, which is 22.1 % higher than that of the single air-staging.

Keywords: gas boiler, nitrogen reduction, staged combustion, humidification combustion, compound combustion.

Introduction

Gas boilers play an important role in contributing to NO_x emissions, making No_x reduction technologies crucial in the combustion process. Consequently, various combustion technologies have been rapidly developed to reduce NO_x emissions Nemitallah et al., 2018 [1]. These technologies include premixed combustion [2], humidification combustion [3], air-staged combustion [4], flue gas recirculation [5], and flameless combustion [6]. However, issues such as flame tilt and combustion instability have limited the efficiency of nitrogen reduction in premixed combustion and flue gas recirculation technologies, leading to increased incomplete combustion losses Liang et al., 2019 [7]. Existing flameless combustion technologies require additional dilution or preheating of reactants, which also have certain limitations [8–10].

Air-staged combustion technology has shown promising results in the utilization of coal-fired boilers [11–13]. Xu et al. [14] achieved a reduction in NO concentration, decreasing it from 142.97 mg/m³ to 108.22 mg/m³ using air-staged combustion technology. Y. Wang et al. [12] found that deep air-staged combustion exhibited superior NO_x reduction performance compared to shallow air-staged combustion. Wu et al. [15] simulated the NO_x emission of gas boiler under different primary air ratios. Reducing the primary air ratio in the range of 0.7–0.85 can effectively reduce NO_x emissions. Q. Wang et al. [18] implemented a novel air-staged low-NO_x combustion technique by varying the ratio between the secondary air ratio and the staged air ratio in the burner. As the level of air-staged in the furnace increased, the NO_x emissions consistently decreased. At the optimal secondary air ratio/staged air ratio of 47.1/13.5, the No_x reduction efficiency reached approximately 46 %. Regarding the characteristics of NO formation and reduction in the air-staged combustion process, there have been numerous studies [17–21]. The results indicate that NO_x emissions are mainly influenced by combustion temperature, reducing gases, and residence time. In a low-oxygen highly reducing atmosphere, the NO concentration can be effectively suppressed [19, 20]. Low-temperature combustion not only reduces the emissions of NO_x but also helps in reducing fuel consumption (Pachiannan et al., 2019) [21]. In addition, introducing steam during the combustion process can also contribute to reducing NO_x emissions [22]. Miyauchi et al. [23] found that increasing air humidity lowers the concentration of NO when the flame's maximum temperature remains constant. Lee et al. [24] successfully reduced NO_x emissions from gas boilers by injecting water into the combustion process. Minakov et al. [25] found that in liquid hydrocarbon combustion, No_x production decreased significantly with increasing vapor flow. Tian et al. [26] further demonstrated that a 50 % gas-to-water rate resulted in a 75 % reduction in NO_x emissions compared to dry conditions. Kapusuz et al. [3] proposed that increasing air humidity from 35 % to 80 % could achieve a NO_x removal efficiency of 53 %. Yogeewara et al. [27] conducted a study on diesel engines and found that the maximum NO_x emission occurred at approximately 958 mg/m³ under 80 % relative humidity. Co-combustion of coal-water slurry as a reducing agent with pulverized coal reduced NO emissions by 47 % by Alekseenko et al. [28]. However, since 2014, the

ultra-low emission standards require NO_x levels to be no more than 50 mg/m^3 (with 6 % O_2 content) [29]. Single nitrogen reduction techniques may not be sufficient to meet the emission reduction requirements, and the combination of multiple nitrogen reduction technologies could potentially achieve better nitrogen reduction performance [30–32]. Cozzi et al. [30] combined air-staged combustion with premixed combustion to significantly reduce the levels of nitrogen emissions as low as 5 mg/m^3 . Houshfar et al. [31] found that an integrated system combining air-staged combustion and flue gas recirculation can further reduce NO_x emissions by an additional 5 %–10 % compared to air-staged combustion alone. Tian et al. [32] combined air-staged combustion, premixed combustion, and flue gas recirculation, resulting in better nitrogen reduction performance compared to conventional combustion, achieving a 72 % reduction in nitrogen emissions. Humidification has been found to be an efficient method to reduce nitrogen emissions. To the best of our knowledge, there are very few studies on the combination of air-staged and humidification techniques, especially for natural gas. And there is limited sensitivity analysis on the main reactions involved in NO formation during the combustion process. Therefore, this article aims to investigate the nitrogen reduction effect through the combination of air-staged and humidification technology. Sensitivity analysis of NO will be conducted to explore its formation characteristics. Due to experimental limitations, many researchers [33–35] have utilized CHEMKIN software to study the formation characteristics of NO_x during fuel combustion and variations in reactants. Wang et al. [35] employed CHEMKIN to investigate the influence of combustion temperature and other factors on the migration of fuel nitrogen in the main combustion zone (MCZ). S. Wu et al. [36] utilized two plug flow reactor (PFR) models to study the NO_x emission characteristics of air-staged combustion under high-temperature, highly reducing atmospheres. Some researchers [37] combined the PFR and perfectly stirred reactor (PSR) models to simulate the air-staged combustion and obtained satisfactory simulation results.

Based on the literature reviewed above, this study used CHEMKIN software to numerically investigate the nitrogen reduction performance and NO sensitivity analysis in different compound modes of air-staged and humidification combustion. The research focused on investigating the influence of combustion temperature, excess air coefficient, and injection position of over-fire air on the nitrogen reduction performance of air-staged and humidification combustion. The simulation results indicate that the compound technique of humidifying both combustion zones achieves the best nitrogen reduction effect, surpassing the nitrogen reduction rate of single combustion techniques. This study provides theoretical guidance for reducing NO_x emissions in actual gas boiler exhaust gases.

1. Physical model

Figure 1a shows the physical diagram of a 1.4 MW gas boiler. The height of the furnace is 4.36 m, and the horizontal cross section of the furnace is rectangular with the width of 2.15 m and the depth of 1.75 m. There are two pipes with the diameter of 0.4 m at both the top and the bottom of the boiler. The bottom pipe serves as the inlet for fuel and combustion air and the top as the outlet for flue gas. Additionally, on the right side of the furnace, there is the inlet for over-fire air with the diameter of 0.3 m.

Figure 1b illustrates the schematic diagram of air-staged combustion, while Figure 1c represents the schematic diagram of humidification combustion. The difference lies in the composition of the combustion air and whether it is introduced in the graded manner into the boiler. In air-staged combustion, fuel and a small amount of combustion air enter the MCZ from the bottom inlet of the boiler. At the inlet of the burnout zone on the right side of the boiler, secondary air is introduced to achieve air-staged combustion in different proportions. In humidification combustion, fuel, combustion air, and water enter the MCZ from the bottom inlet, without a secondary air inlet. The combustion products are directly exhausted from the top outlet of the boiler. Figure 1d depicts the schematic diagram of the compound combustion technology, which combines the above two combustion methods. Building upon air-staged combustion, this approach involves introducing water into different combustion zones to achieve compound humidification. Fuel, combustion air, and water are supplied to the boiler from the bottom inlet, while over-fire air is supplied to the right-side inlet of the boiler for staging combustion. This represents compound humidification in the MCZ. When fuel and combustion air enter the boiler from the bottom inlet, and water and over-fire air enter from the right-side inlet, this represents compound humidification in the burnout zone. Figure 1d shows compound humidification occurring in both the MCZ and the burnout zone. Based on air-staged combustion, water is introduced into the boiler for combustion through both the bottom and the right-side inlets.

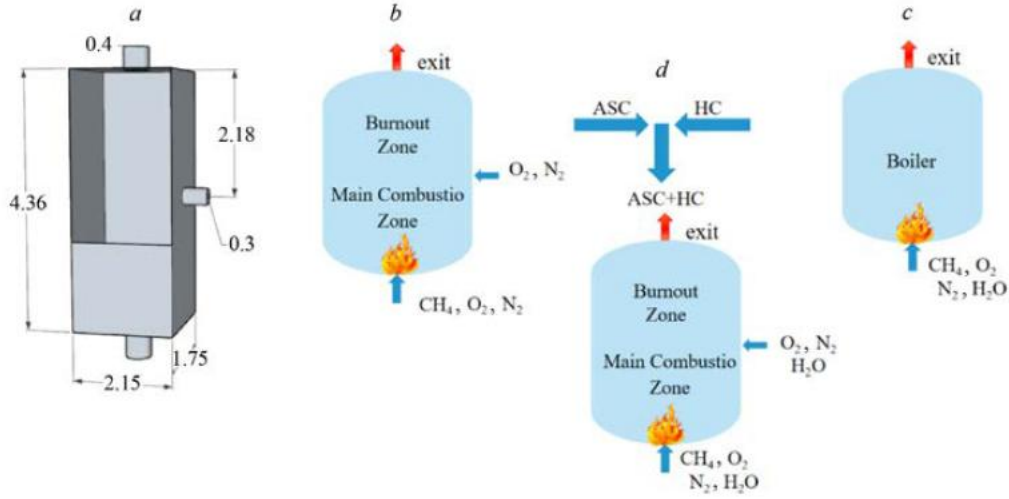


Fig. 1. Physical diagram (a) of gas boiler and schematic diagram (b, c, d).
Dimensions are given in meters.

The nitrogen reduction principle of air-staged combustion technology involves introducing staged combustion air into the furnace. In the MCZ, only a small amount of combustion air is injected to cause fuel excess and incomplete combustion. At this point, the MCZ is predominantly reducing in nature, and the lack of oxygen accelerates the reduction of NO_x generated by NH_n ($n = 0, \dots, 3$) and CH_m ($m = 1, \dots, 4$) to N_2 [37]. Additionally, the reduction in furnace temperature also reduces the formation of NO_x . Subsequently, the introduction of over-fire air in the burnout zone achieves complete combustion and reduces the emission of NO_x . The nitrogen reduction principle of humidification combustion technology lies in increasing the concentration of water in the furnace through the humidification process, thereby diluting the concentrations of N_2 and oxidants [38]. The heat absorption process of water in the furnace lowers the combustion temperature, effectively suppressing the formation of NO_x .

This paper combines the above two combustion technologies. Under the reducing atmosphere established by air-staged combustion, the combustion temperature is reduced through water evaporation, effectively achieving the deep nitrogen reduction.

2. Mathematical model

2.1. Mathematical equation

The one-dimensional PFR is an ideal reactor. The governing equations are as follows: Mass conservation equation:

$$\rho u \frac{dF}{dx} + \rho F \frac{du}{dx} + uF \frac{d\rho}{dx} = 0, \quad (1)$$

where ρ is the density, kg/m^3 ; u is the speed, m/s ; F is the cross-sectional area of PFR reactor, m^2 ; x is the length of PFR reactor, m .

Gas phase transformation equation:

$$\rho u F \frac{dX_k}{dx} = W_k \omega_k F, \quad (2)$$

where X_k is the mass fraction of gas k at the outlet; W_k is the molecular weight of the k th substance; ω_k is the production rate of the k th substance, $\text{mg}/(\text{m}^3 \cdot \text{s})$.

Energy conservation equation:

$$\rho u F \sum_{k=1}^{k_g} h_k \frac{dX_k}{dx} + c_p \frac{dT}{dx} + u \frac{du}{dx} = B_e Q_e, \quad (3)$$

where h_k is the enthalpy of the k th substance, kJ/kg; c_p is the specific heat capacity at constant pressure, kJ/(kg·K); T is the temperature, K; B_e is the surface area, m²; Q_e is the heat flux, W/m².

2.2. Reactors and models

Figure 2a shows that all the gas components flow in parallel after the fuel and air enter the reactor from the inlet. The model assumes complete mixing of the fuel and oxidizer entering the PFR, neglecting the influence of mixing efficiency on the reaction. Parameters such as temperature, pressure, and flow rate are assumed to be radially constant but vary along the axial direction of flow. It is assumed that the premixed gas reaches the desired inlet reaction temperature before entering the simulated reactor, neglecting the effects of the temperature rise at the inlet.

The actual combustion process of a gas boiler is assumed to consist of two PFR models. In Fig. 2, each model has a length of 50 cm and a diameter of 20 cm. The PFR1 model simulates the MCZ of the boiler, while the PFR2 model simulates the burnout zone of the boiler. The combustion air and fuel enter from the inlet of PFR1 model, while the over-fire air enters from the inlet of PFR2 model. After the reactions, the gases leave through the outlet.

2.3. Boundary conditions

Both PFR models are adiabatic and do not affect each other. The inlet temperature of the MCZ is set to 1800 K, while the inlet temperature of the burnout zone is set to 1700 K. The excess air coefficient of the furnace is set to 1. The fuel is all considered as methane, and the gas dynamics standard methane oxidation mechanism GRI-3.0 is used to simulate the effect of NO formation in the compound mode of boiler combustion.

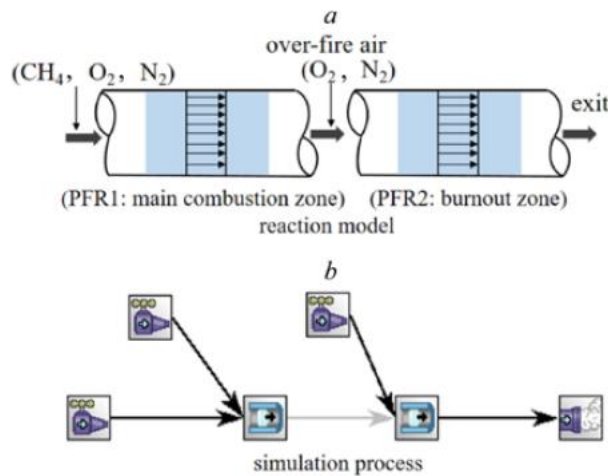


Fig. 2. Air-staged and humidification combustion model.

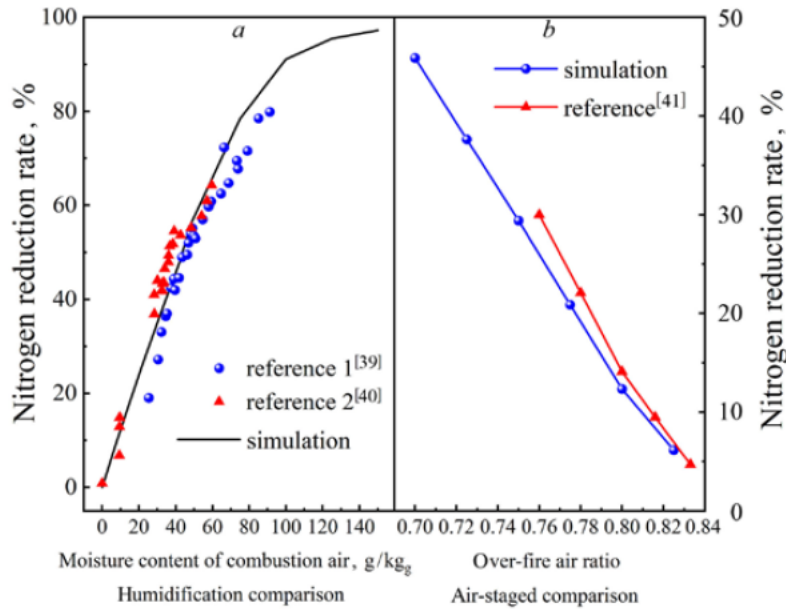


Fig. 3. Model verification.

2.4. Model verification

Figure 3 illustrates the accuracy of the PFR model simulation results. The nitrogen reduction rates obtained from the humidification combustion experiments conducted by D. Sun [39] and H. Zhai [40] are compared with the simulated nitrogen reduction rates. The error between the experimental and simulated nitrogen reduction rates does not exceed 5 %, and their trends are consistent. In this simulation, the nitrogen reduction rate of air-staged combustion is compared with the reduction rate studied by B. Sun et al. [41]. The error is less than 8 %, with consistent trends. Therefore, the results of the PFR model in the qualitative study of NO emissions and the variation of air-staged combustion and humidification combustion are credible.

3. Results discussion

3.1. Influence of different combustion modes on nitrogen reduction performance and sensitivity analysis

Figure 4 shows the axial distribution of NO mole fraction under different over-fire air rates during air-staged combustion. After the fuel and combustion air enter the MCZ, the NO mole fraction rapidly increases with the increasing axial distance and then tends to stabilize. After injecting over-fire air for a certain period of time, the NO mole fraction at the inlet of the burnout zone rapidly decreases. With the increase of over-fire air rate, the NO mole fraction decreases. As the combustion proceeds, the amount of oxygen in the MCZ becomes insufficient. The reductive products such as CO and H₂ produced in the MCZ increase, enhancing the reductive atmosphere in the MCZ. In Fig. 4 and Fig. 5, when over-fire air rate is 30 %, the NO mole fraction is 17 % lower than that without air-staged combustion. And the CO mole fraction in the MCZ is 148 % higher than that without air-staged combustion. By changing the rate of over-fire air, the intermediate products CO and H₂ in the MCZ are affected, thereby changing the reductive atmosphere in the MCZ and reducing the NO mole fraction at the outlet, effectively reducing the NO emissions during the combustion process.

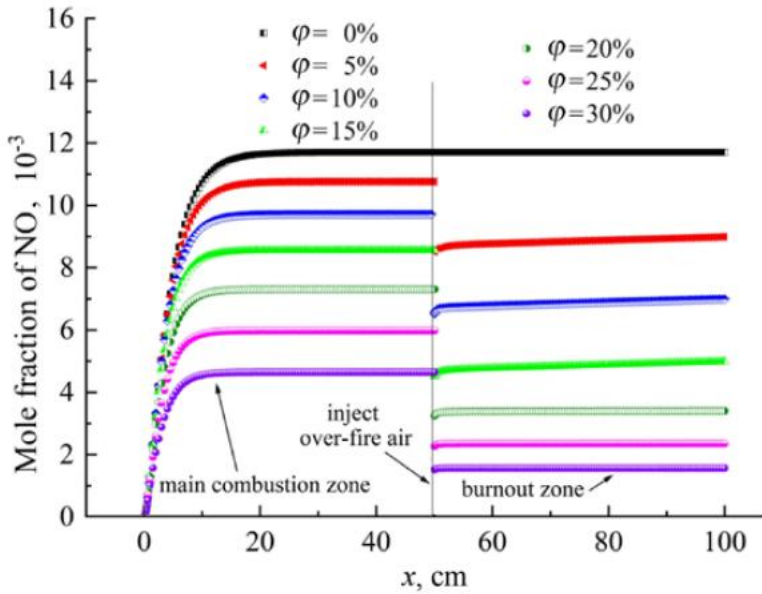


Fig. 4. Influence of over-fire air rate on NO mole fraction.

A sensitivity analysis was conducted on the NO formation in air-staged combustion to further understand the characteristics of NO formation. Figure 6 shows the reactions affecting NO formation and key locations. The sensitivity of reactions in the MCZ is higher than in the burnout zone. At axial distances of 10 cm and 17 cm in the MCZ, R53 and R158 inhibit NO formation, while other reactions promote NO formation. Additionally, as axial distance increases, the sensitivity of reactions influencing NO formation decreases. At 50 cm, no NO formation occurs. In the burnout zone, all reactions promote NO formation, with R178 exhibiting higher sensitivity and forming thermal NO.

Therefore, in the MCZ under the reducing atmosphere of air-staged combustion, the formation of prompt NO is mainly promoted. In the burnout zone, where there is sufficient oxygen, thermal NO is promoted. However, due to fuel and over-fire air rate restrictions in the burnout zone, NO formation is limited, ultimately leading to a reduction in NO formation in air-staged combustion.

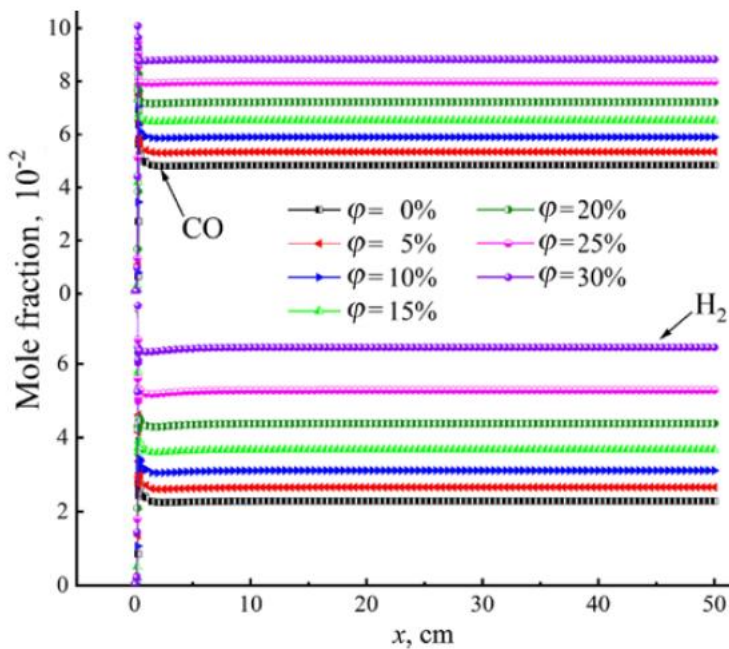


Fig. 5. Influence of over-fire air rate on CO and H₂ mole fraction.

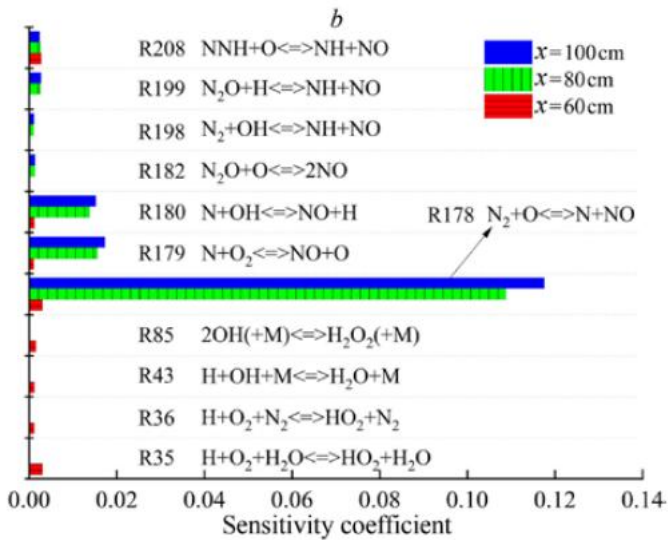
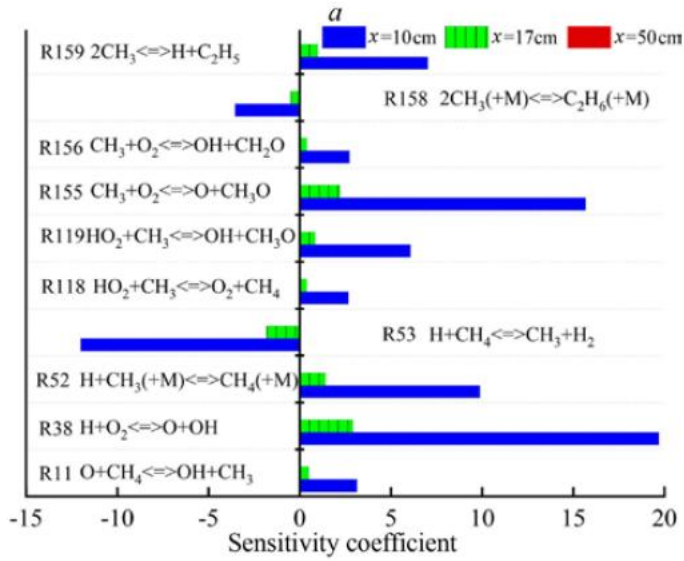


Fig. 6. Sensitivity analysis of NO formation ($\varphi = 10\%$).
Main combustion zone (a), burnout zone (b).

Therefore, in the MCZ under the reducing atmosphere of air-staged combustion, the formation of prompt NO is mainly promoted. In the burnout zone, where there is sufficient oxygen, thermal NO is promoted. However, due to fuel and over-fire air rate restrictions in the burnout zone, NO formation is limited, ultimately leading to a reduction in NO formation in air-staged combustion.

3.1.2. Nitrogen reduction performance of air-staged and humidification combustion

Based on air-staged combustion ($\varphi = 15\%$), air entering the combustion zone is humidified, with the humidity content gradually increasing from 0 to 48 g/kgg (see Figs. 7 and 8). Figures 7a and 7b show NO mole fractions in different combustion zones after individual and both humidification, respectively. As humidity content increases, the molar fraction of NO at the outlet decreased and the nitrogen reduction rate increased linearly for each of the different combustion zones after humidification. In Fig. 7a, humidification of the MCZ only leads to a maximum reduction in the molar fraction of NO by 12%. The difference in NO mole fraction between different humidity contents in the burnout zone is smaller than that in the MCZ. After humidifying only the burnout zone in Fig. 7a, the reaction between O₂ and N₂ at high temperature results in a rapid increase in the molar fraction of NO. However, after a certain distance, the decrease in O₂ leads to a slower rate of NO

formation. Additionally, the rate of increase of NO molar fraction slows down with increasing humidity for different cases of humidification of the combustion zone.

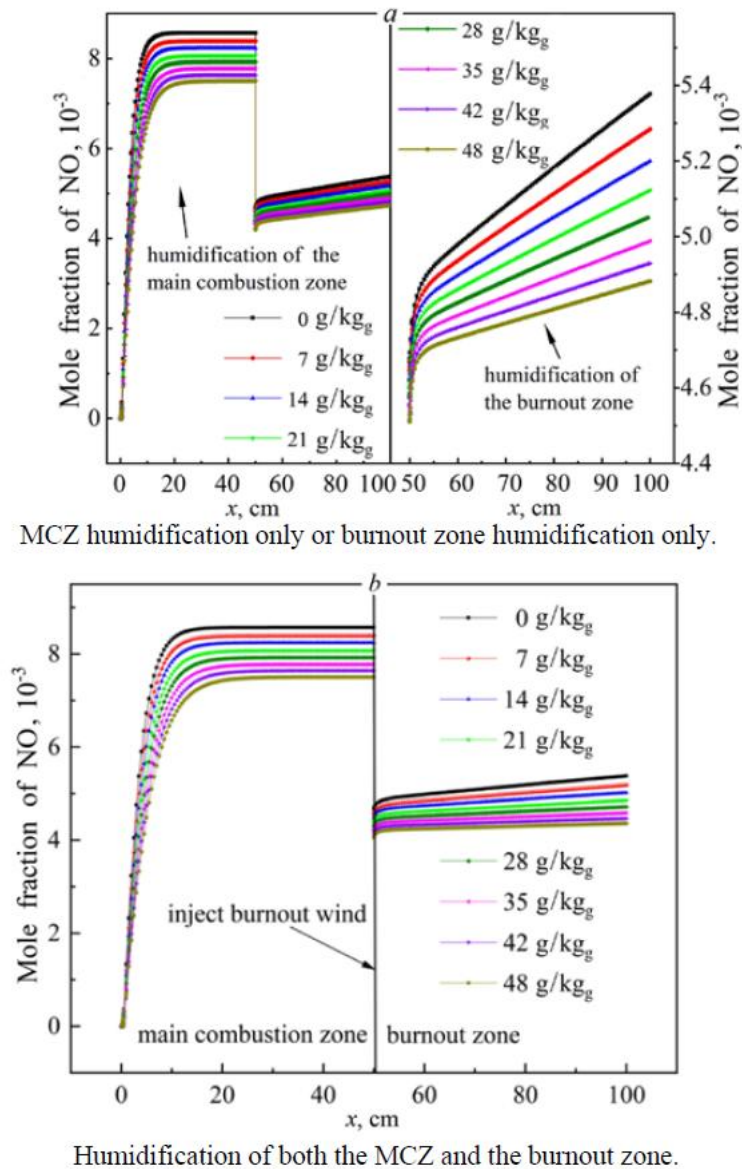


Fig. 7. Effects of air humidity on NO mole fraction.

Figure 8 illustrates the nitrogen reduction rate of compound combustion increases linearly with the increase of humidity content. The nitrogen reduction rate of both the MCZ and the burnout zone is higher than that of the single zone. Moreover, the impact of humidity content on the nitrogen reduction rate becomes more significant as it increases. At 48 g/kg_g, the molar fraction of NO at the outlet of the burnout zone decreases from 5·10⁻³ to 4.3·10⁻³ at most. Compared to air-staged combustion alone, the maximum nitrogen reduction rate increases by 7.4%. On the basis of air-staged combustion, humidifying both combustion zones is more advantageous in reducing NO formation and improving the nitrogen reduction rate.

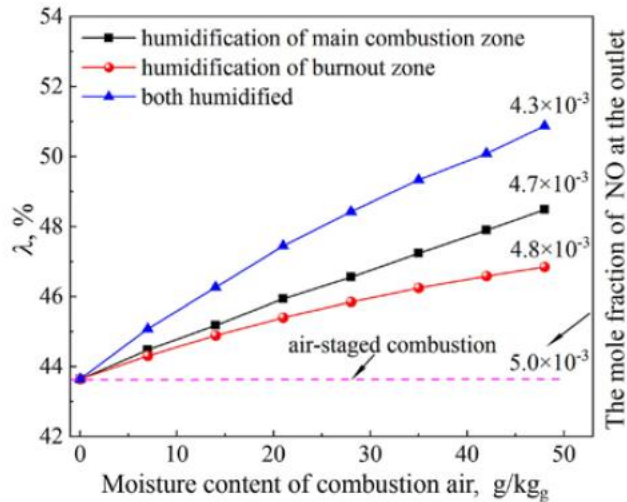


Fig. 8. Effect of moisture content of combustion air on nitrogen reduction rate and outlet NO mole fraction.

3.1.3. NO sensitivity analysis of air-staged and humidification combustion

The MCZ is selected at 0.5 cm, and positions at 50.5 cm and 100 cm are chosen in the burnout zone for NO sensitivity analysis in air-staged and humidification combustion. Figure 9 shows the humidification in the MCZ inhibits R119. Additionally, during the humidification process, the concentration of OH increases, further enhancing the inhibition of NO formation through R119. Sensitivity coefficients indicate that promoting R53 has a good inhibitory effect on NO formation, while the other reactions promote NO formation. R52, R38, and R155 exhibit higher sensitivity coefficients, indicating more significant promotion effects. The air-staged and humidification in the MCZ have both the promotion and inhibition effects on NO formation.

Figure 10 depicts R35, R36, R99, and R208 affect NO formation at 50.5 cm. Increasing humidity content enhances the sensitivity of R35 and R99, promoting NO formation, while reducing the sensitivity of R36 and R208 inhibits NO formation. At 100 cm, R35 inhibits NO formation, while the other reactions promote NO formation. The sensitivity coefficient of R178 is relatively large, but lower than that of individual air-staging. When humidity content increases to 48 g/kgg, the sensitivity coefficient of R178 decreases to 41 % of its original value. As humidity content increases, the sensitivities of R182, R185, and R199 gradually decrease to 0. Both air-staged and humidification in the MCZ and the burnout zone contribute to the reduction of sensitivity coefficients of certain reactions, leading to a decrease in NO molar fraction at the combustion zone exit and an improvement in nitrogen reduction rate.

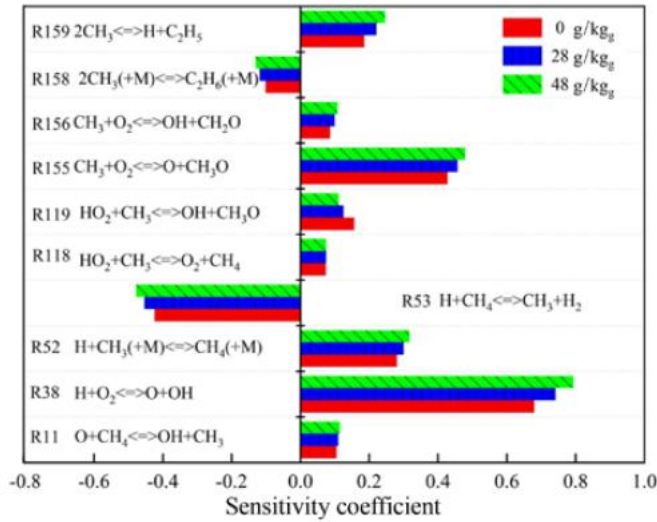


Fig. 9. Sensitivity analysis of NO formation in the MCZ ($x = 0.5$ cm).

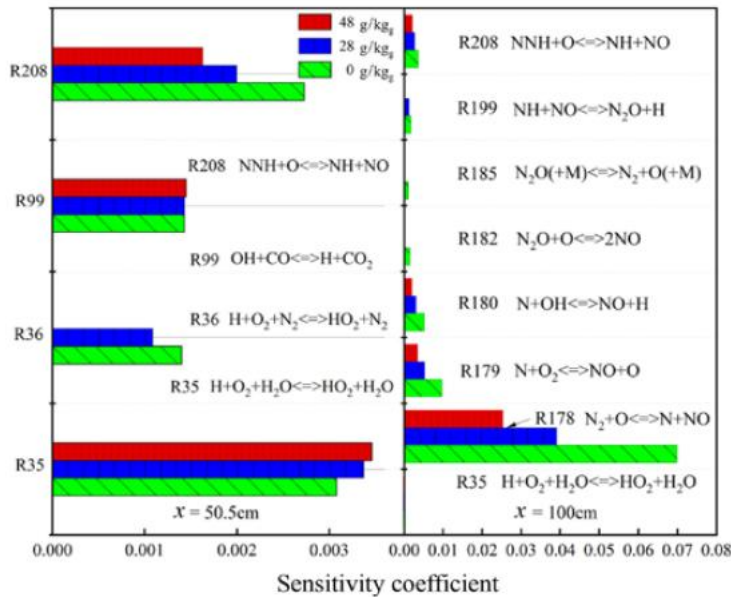


Fig. 10. Sensitivity analysis of NO formation in the burnout zone.

3.2. Influencing factors on nitrogen reduction performance in compound mode

The combined humidification of MCZ and burnout zone only leads to a 7.4% increase in nitrogen reduction rate. During the humidification process, nitrogen reduction rate is also influenced by other factors. Therefore, the impact of different combustion temperature, excess air coefficient, and the positions of over-fire air on nitrogen reduction performance was further simulated under the optimal compound nitrogen reduction mode.

3.2.1. Effect of combustion temperature on nitrogen reduction performance in compound mode

The influence of different combustion temperature on nitrogen reduction rate was considered based on the constant gas and air temperatures. Specifically, the temperatures in the MCZ and the burnout zone decrease from 1800 and 1700 K, respectively, to 1500 and 1400 K. Figure 11 shows the NO concentration increases rapidly and then stabilizes with increasing axial distance.

As the combustion temperature decreases, the NO molar fraction and generation rate at the boiler outlet also decrease. At the exit of the MCZ and the burnout zone, the NO molar fraction corresponding to a combustion

temperature of 1800 K is 43 % and 33 % higher than that at a combustion temperature of 1500 K, respectively. Changing the combustion temperature has a greater impact on the NO concentration in the MCZ than in the burnout zone. Lowering the combustion temperature can further reduce the formation of NO. The nitrogen reduction rate increases linearly based on a 51 % reduction in NO. When the temperatures T_1 and T_2 decrease to 1500 and 1400 K, respectively, the nitrogen reduction rate increases to 65.7 %, which is 22.1 % higher than that of the air-staged combustion.

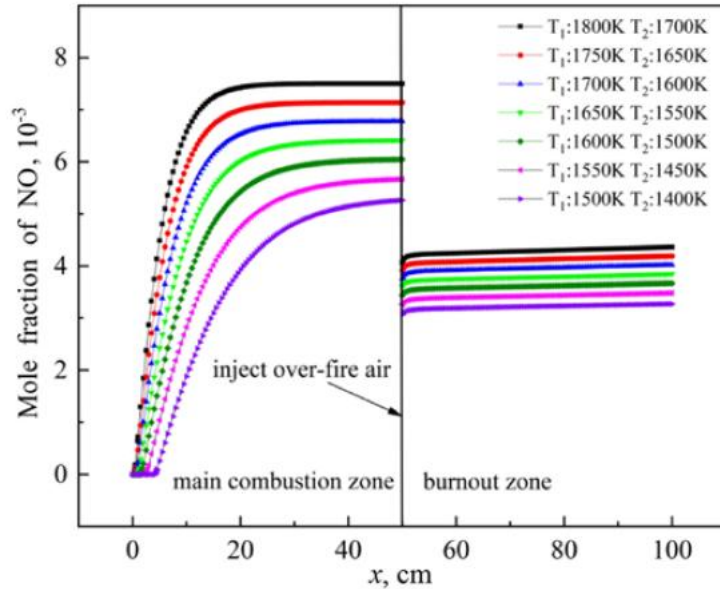


Fig. 11. Effects of different temperature conditions on NO mole fraction.

Figure 11 illustrates changing the temperature of combustion zones has a significant impact on the mole fraction of NO in the MCZ. Therefore, the influence of the temperature in the MCZ on the nitrogen reduction rate was studied separately. Set T_2 to 1400 K and change T_1 . Figure 12 depicts the impact of different humidity content values on the nitrogen reduction rate. As T_1 increases, the nitrogen reduction rates for different humidity levels consistently decrease. When T_1 is constant, an increase in humidity content leads to an improvement in the nitrogen reduction rate. Different levels of humidity in the combustion air result in varying rates of change in the nitrogen reduction rate with increasing T_1 . For 0 g/kg, as T_1 increases, the rate of decrease in the nitrogen reduction rate gradually slows down. When T_1 increases from 1500 to 1600 K, the nitrogen reduction rate decreases by 11 %. However, when T_1 increases from 1700 to 1800 K, the nitrogen reduction rate decreases by 4.9 %. For 48 g/kg, as T_1 increases, the rate of decrease in the nitrogen reduction rate gradually accelerates. When T_1 increases from 1500 to 1600 K, the nitrogen reduction rate decreases by 4.2 %. However, when T_1 increases from 1700 K to 1800 K, the nitrogen reduction rate decreases by 7.2 %.

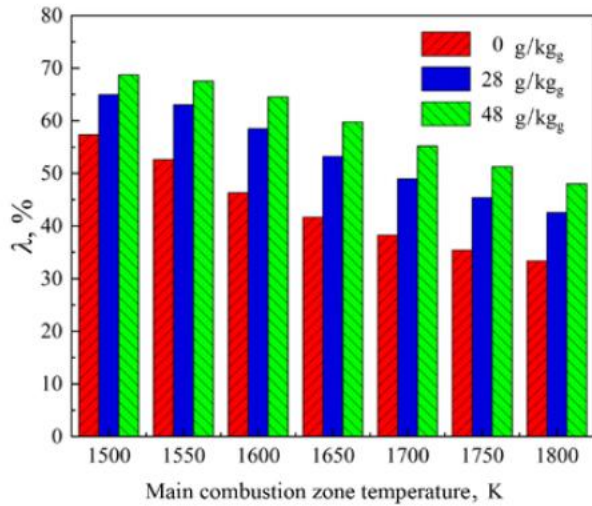


Fig. 12. Effect of MCZ temperature on nitrogen reduction rate.

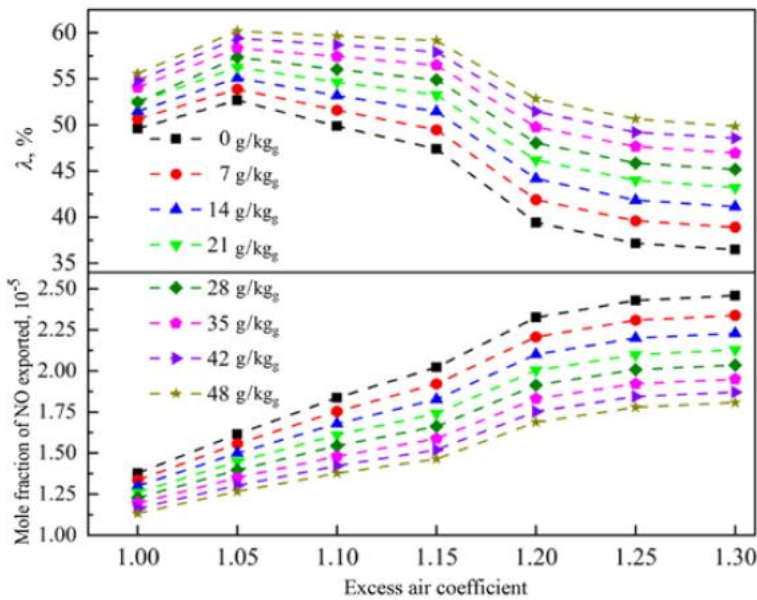


Fig. 13. Effect of excess air coefficient on outlet NO mole fraction and nitrogen reduction rate under compound mode.

3.2.2. Effect of excess air coefficient on nitrogen reduction performance in compound mode

Figure 13 shows the NO molar fraction at the exit of the burnout zone under different excess air coefficient. As the excess air coefficient increases, the NO molar fraction at the exit of the burnout zone gradually increases, while increasing humidity content leads to a decrease in the NO molar fraction. When humidity content is constant, increasing excess air coefficient initially increases the nitrogen reduction rate of air-staged and humidification. But it decreases after reaching a maximum at 1.05. Therefore, increasing excess air coefficient appropriately can improve nitrogen reduction efficiency. With the increase of humidity content, the degree of reduction in nitrogen reduction rate gradually decreases. At 0 g/kg, excess air coefficient increases to 1.3, and the nitrogen reduction rate decreases by 13.1 %, while at 48 g/kg, the nitrogen reduction rate only decreases by 5.7 %. Increasing excess air to improve nitrogen reduction rate, while considering air humidification, is more favorable for reducing the emission of NO during combustion.

3.2.3. Effect of over-fire air position on nitrogen reduction performance in compound mode

The MCZ is a reducing atmosphere, so the length of stay in the MCZ will affect the formation of NO. Changing the injection position of the combustion air can change the length of stay in the MCZ. Figure 14 shows that when T_1 is 1800 K and T_2 is 1400 K, the residence time increases linearly with the increase of MCZ length. When the length of the MCZ increases from 40 cm to 64 cm, the residence time increases from 0.93 s to 1.49 s. The reduction reaction of NO reduces the molar fraction of NO at the outlet, increasing the reduction rate of nitrogen. When the length of MCZ decreases from 64 cm to 40 cm, nitrogen reduction rate decreases by 2.94 % at 48 g/kgg, which is 1.96 % lower than that at 0 g/kgg. Increasing humidity content also effectively improves the nitrogen reduction rate, thereby mitigating the negative impact of shortening the length of the MCZ.

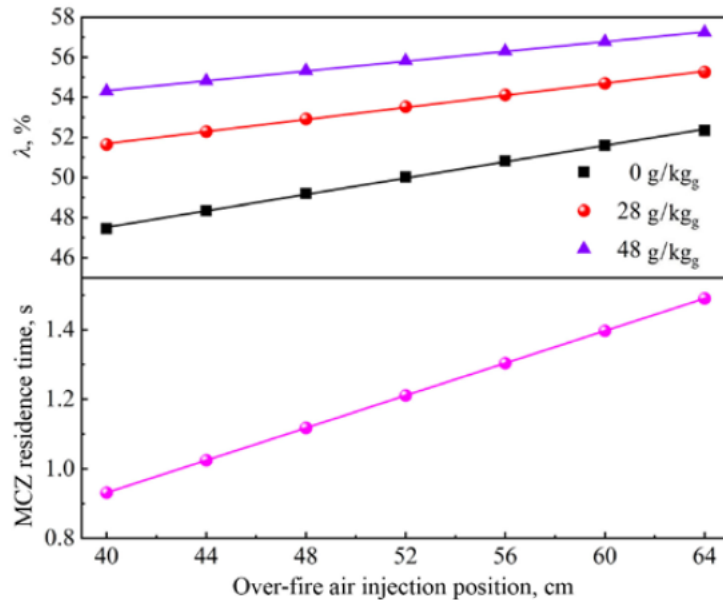


Fig. 14. Effect of injection position of over-fire air on nitrogen reduction rate and residence time of the MCZ in compound mode.

In addition, both turbulence intensity and swirl intensity are velocity-dependent and are key factors in controlling the flue gas emission and combustion efficiency, especially the control of swirl in combination with air-staged can achieve low NO and high embers combustion. A number of studies have found that the swirl intensity of pulverized coal burners has a significant effect on NO_x emissions [45]. Higher swirl results in faster mixing of fuel and air, which reduces the flame temperature level and decreases thermal NO emissions [46]. Ikeda et al [47] showed that optimizing the swirl intensity of the secondary air reduces NO emissions. In air-staged and humidification combustion, changing the direction of the main swirl flow contributes to the intensive mixing of fuel and oxidizer. The change in operation leads to a reconfiguration of the flow pattern and the formation of a multi-vortex flow structure. The increase in the residence time of coal particles in the combustion chamber reduces the combustible losses from 1.9 % to 0.51 % [28].

3.3. Comparison of combustion technologies

In Table, the different nitrogen reduction combustion technologies are arranged in ascending order based on their optimal nitrogen reduction rates. The proposed air-staged and humidification combustion technology achieves the highest nitrogen reduction rate of 65.7 %, with T_1 set at 1500 K and T_2 at 1400 K. Among the five individual nitrogen reduction technologies considered, humidification combustion exhibits the highest reduction rate, but it is 12.7 % lower than that of air-staged and humidification combustion. The air-staged combustion follows with a nitrogen reduction rate as high as 45 %, but it has a 20.7 % lower nitrogen reduction rate compared to air-staged and humidification combustion. Under the same combustion technology, compound combustion shows better nitrogen reduction performance compared to individual combustion techniques. Oxy-fuel combustion has the lowest nitrogen reduction rate at 36.7 %. The nitrogen reduction rates of air-staged and humidification combustion are 29 % higher than that of oxy-fuel combustion, highlighting superior nitrogen reduction performance. Overall, the comprehensive analysis indicates that air-staged and humidification combustion technology outperforms individual nitrogen reduction combustion technologies.

Table

Comparison of nitrogen reduction effects of different nitrogen reduction combustion technologies

Research object	Combustion technology	Nitrogen reduction rate, %	Ref.
CFB combustion chamber	oxy-fuel combustion	36.7	[42]
waste incineration power plant	flue gas recirculation	39.8	[43]
methane(40 %N ₂)	premixed combustion	44.4	[44]
gas boiler ($\phi = 15\%$)	air-staged combustion	45	-
SI engine	humidification combustion	53	[3]
gas boiler	air-staged + humidification combustion	65.7	-

Conclusions

This study simulated and investigated the nitrogen reduction performance of a gas boiler and NO sensitivity analysis under different air-staged and humidification methods. The influence of combustion temperature, excess air coefficient, and the position of over-fire air on the nitrogen reduction performance was analyzed. The nitrogen reduction rates of different combustion methods were compared. The simulation results are as follows: (1) Air-staged combustion creates a reducing atmosphere in the MCZ, mainly leading to the formation of prompt NO, while the burnout zone promotes the formation of thermal NO. The optimal ratio of over-fire air is between 5% and 15%. (2) When both the MCZ and the burnout zone are humidified, the nitrogen reduction rate reaches 51%, surpassing that of other combustion methods. Further reduction of T1 and T2 can increase the nitrogen reduction rate up to 65.7%. (3) The nitrogen reduction rate is more favorable when the excess air coefficient is between 1.0 and 1.1. The best nitrogen reduction effect is achieved when excess air coefficient is 1.05. (4) Shortening the length of the MCZ will result in a linear decrease the nitrogen reduction rate. When humidity content is 48 g/kg, reducing the length of the MCZ from 64 cm to 40 cm will lead to a decrease in the nitrogen reduction rate by 2.94%. (5) The compound air-staged and humidification technique achieved a higher nitrogen reduction rate compared to the individual air-staged combustion and humidification combustion techniques, with an additional increase of 20.7% and 12.7%, respectively.

Nomenclature

Abbreviations

MCZ — Main Combustion Zone,
PSR — Perfectly Stirred Reactor

PFR — Plug Flow Reactor.
CHEMKIN — Chemical Kinetics

Symbols

B_e — surface area, m²,
 c_p — specific heat capacity at constant pressure, kJ/(kg·K)
 F — cross-sectional area of PFR reactor, m²,
 h_k — enthalpy of the k th substance, kJ/kg,
 Q_e — heat flux, W/m²,
 T — temperature, K,
 u — speed, m/s,

W_k — molecular weight of the k th substance,
 X_k — mass fraction of the k th gas at the outlet,
 x — length of PFR reactor, m,
 ρ — density, kg/m³,
 λ — nitrogen reduction rate,
 ϕ — over-fire air rate,
 ω_k — production rate of the k th substance, mg/(m³·s).

Consent to participate

Informed consent was obtained from all individual participants included in the study.

Funding

This work was supported by the BUCEA Doctor Graduate Scientific Research Ability Improvement Project (Grant numbers [DG2023010])

Conflict of interest

The authors have no competing interests to declare that are relevant to the content of this article.

Data availability statement

The data sets generated and supporting the findings of this article are obtainable from the corresponding author upon reasonable request. The authors attest that all data for this study are included in the paper. Data provided by a third party are listed in acknowledgment.

Author contributions

All authors contributed to the study conception and design. Material preparation, data collection and analysis were performed by [Q. Zhang], [Y. Guo], [T. Liu], [W. Zhao], [S. Qiu] and [X. Lü]. The first draft of the manuscript was written by [Y. Guo] and all authors commented on previous versions of the manuscript. All authors read and approved the final manuscript.

References

1. **M.A. Nemitallah, S.S. Rashwan, I.B. Mansir, A.A. Abdelhafez, and M.A. Habib**, Review of novel combustion techniques for clean power production in gas turbines, *J. Energy Fuels*, 2018, Vol. 32, No. 2, P. 979–1004.
2. **F. Liu, L. Zheng, and R. Zhang**, Emissions and thermal efficiency for premixed burners in a condensing gas boiler, *J. Energy*, 2020, Vol. 202, P. 117449.
3. **M. Kapusuz, A. Cakmak, and H. Ozcan**, Emissions analysis of a SI engine with humidified air induction, *J. Energy Procedia*, 2018, Vol. 147, P. 235–241.
4. **X. Qi, M. Yang, and Y. Zhang**, Numerical analysis of NO_x production under the air staged combustion, *J. Frontiers in Heat and Mass Transfer*, 2017, Vol. 8.
5. **M. Abdelaal, M. El-Riedy, A.M. El-Nahas, and F.R. El-Wahsh**, Characteristics and flame appearance of oxyfuel combustion using flue gas recirculation, *J. Fuel*, 2021, Vol. 297, P. 120–775.
6. **W. Liu, Z. Ouyang, X. Cao, and Y. Na**, Experimental research on flameless combustion with coal preheating technology, *J. Energy Fuels*, 2018, Vol. 32, P. 7132–7141.
7. **X. Liang, Y. Wang, H. Yu, H. Zhang, and Z. Zheng**, A review of early injection strategy in premixed combustion engines, *J. Applied Sciences*, 2019, Vol. 9, P. 3737.
8. **D. Yang and Q.W. Chen**, The discharge status and technical analysis of NO_x of thermal power plant boiler, in: *APPL. MECH. MATER.*, Trans Tech Publications Ltd, 2014, Vol. 535, P. 131–134.
9. **I. Oluwoye, Z. Zeng, S. Mosallanejad, M. Altarawneh, J. Gore, and B. Dlugogorski**, Controlling NO_x emission from boilers using waste polyethylene as reburning fuel, *Chem. Eng. J.* 2021, Vol. 411, P. 128427.
10. **J. Park, D. Kim, and Y. Lee**, Experimental study on flameless combustion and NO emission with hydrogen-containing fuels, *Inter. J. Energy Res.*, 2022, Vol. 46, P. 2512–2528.
11. **Q. Wang, Z. Chen, J. Wang, L. Zeng, X. Zhang, X. Li, and Z. Li**, Effects of secondary air distribution in primary combustion zone on combustion and NO_x emissions of a large-scale down-fired boiler with air staging, *J. Energy*, 2018, Vol. 165, P. 399–410.
12. **Y. Wang, Y. Zhou, N. Bai, and J. Han**, Experimental investigation of the characteristics of NO_x emissions with multiple deep air-staged combustion of lean coal, *J. Fuel*, 2020, Vol. 280, P. 118416.
13. **G. Zhu, Y. Gong, Y. Niu, S. Wang, Y. Lei, and S. Hui**, Study on NO_x emissions during the coupling process of preheating-combustion of pulverized coal with multi-air staging, *J. Cleaner Prod.*, 2021, Vol. 292, P. 126012.
14. **S. Xu, D. Yu, F. Yao, and K. Wang**, Numerical simulation and optimization of CFB boiler furnace with airstaged low NO_x combustion, *J. Prog. Comput. Fluid Dyn*, 2022, Vol. 22, P. 392–410.
15. **J. Wu, K. Zhao, X. Li, M. Wang, and S. Ni**, Numerical study on staged combustion technology in burner of gasfired boiler, *J. Energy Sources Part A*, 2020, P. 1–14.
16. **W. Bai, H. Li, L. Deng, H. Liu, and D. Che**, Air-staged combustion characteristics of pulverized coal under high temperature and strong reducing atmosphere conditions, *J. Energy fuels*, 2014, Vol. 28, No. 3, P. 1820–1828.
17. **J. Yang, R. Sun, S. Sun, N. Zhao, N. Hao, H. Chen, Y. Wang, H. Guo, and J. Meng**, Experimental study on NO_x reduction from staging combustion of high volatile pulverized coals, Part 1, Air staging, *Fuel Process. Technol.*, 2014, Vol. 126, P. 266–275.

18. **Q. Wang, Z. Chen, J. Wang, L. Zeng, X. Zhang, X. Li, and Z. Li**, Effects of secondary air distribution in primary combustion zone on combustion and NO_x emissions of a large-scale down-fired boiler with air staging, *J. Energy*, 2018, Vol. 165, P. 399–410.
19. **S. Liu, W. Fan, J. Chen, and H. Guo**, Establishment of the N₂O and NO prediction model and reveal of the N₂O formation mechanism during air-staged combustion, *J. IND. ENG. CHEM. RES.*, 2022, Vol. 61, P. 6375–6388.
20. **A.P. Singh and A.K. Agarwal**, Low-temperature combustion: an advanced technology for internal combustion engines, *J. Advances in internal combustion engine research*, 2018, P. 9–41.
21. **Z. He, X. Leng, T. Pachiannan, S. Rajkumar, Q. Wang, and W. Zhong**, A literature review of fuel effects on performance and emission characteristics of low-temperature combustion strategies, *J. Appl. Energy*, 2019, Vol. 251, P. 113380.
22. **B. Ge, Y. Tian, and S. Zang**, The effects of humidity on combustion characteristics of a non-premixed syngas flame, *Int. J. Hydrogen Energy*, 2016, Vol. 41, P. 9219–9226.
23. **T. Miyauchi, Y. Mori, and T. Yamaguchi**, Effect of steam addition on NO formation, *J. in: Symp. (Int.) Combust.*, Elsevier, 1981, Vol. 18, P. 43–51.
24. **C.E. Lee, B.J. Yu, D.H. Kim, and S.H. Jang**, Analysis of the thermodynamic performance of a waste-heat recovery boiler with additional water spray onto combustion air stream, *J. Appl. Therm. Eng.*, 2018, Vol. 135, P. 197–205.
25. **A.V. Minakov, I.S. Anufriev, V.A. Kuznetsov, A.A. Dekterev, E.P. Kopyev, and O.V. Sharypov**, Combustion of liquid hydrocarbon fuel in an evaporative burner with forced supply of superheated steam and air to the reaction zone, *J. Fuel*, 2022, Vol. 309, P. 122181.
26. **Y. Tian, S. Zang, and B. Ge**, Experimental investigation on the combustion performance of N₂ dilution in syngas non-premix combustion in humid air conditions, *J. Appl. Therm. Eng.*, 2016, Vol. 107, P.560–564.
27. **T. Yogeewara and A. Kalaiselvane**, Effect of humidified intake air on a turbo-charged DIC engine: Performance and emission analysis, *J. Mater. Today Proc.*, 2022, Vol. 52, P.2213–2217.
28. **S.V. Alekseenko, A.A. Dekterev, L.I. Maltsev, and V.A. Kuznetsov**, Implementation of a three-stage scheme for the co-combustion of pulverized coal and coal-water slurry in an industrial boiler to reduce NO_x emissions, *J. PROCESS SAF ENVIRON*, 2023, Vol. 169, P. 313–327.
29. **S. Xin, Y. Li, C. Hu, and H. Wang**, Discussion on the key technology of modification of desulfurization ultra-low emission in CFB boiler, in: *IOP Conf. Ser.: Earth Environ. Sci*, IOP Publishing, 2019, Vol. 227, P. 052003.
30. **F. Cozzi and A. Coghe**, Effect of air staging on a coaxial swirled natural gas flame, *J. Exp. Therm Fluid Sci.*, 2012, Vol. 43, P. 32–39.
31. **E. Houshfar, R. A. Khalil, T. Løvås, and Ø. Skreiberg**, Enhanced NO_x reduction by combined staged air and flue gas recirculation in biomass grate combustion, *J. Energy fuels*, 2012, Vol. 26, P. 3003–3011.
32. **Y. Tian, S. Lin, X. Liu, X. Zhou, and M. Xu**, Comparative performance assessment of a u-shaped recuperative radiant tube under conventional and MILD combustion modes, *J. Energy Eng.*, 2018, Vol. 3, No. 144, P. 4018028.
33. **P. Glarborg, J.A. Miller, B. Ruscic, and S.J. Klippenstein**, Modeling nitrogen chemistry in combustion, *J. Prog. Energy Combust. Sci.*, 2018, Vol. 67, P. 31–68.
34. **E.C. Okafor, Y. Naito, S. Colson, A. Ichikawa, T. Kudo, A. Hayakawa, and H. Kobayashi**, Experimental and numerical study of the laminar burning velocity of CH₄-NH₃-air premixed flames, *J. Combust. Flame*, 2018, Vol. 187, P. 185–198.
35. **C. Wang, C. Wang, L. Zhao, M. Yuan, P. Wang, Y. Du, and D. Che**, Simulation investigation on NO_x emission characteristics and mechanisms during co-combustion of fossil fuels with different fuel-nitrogen distributions via CHEMKIN, in: *J. Lyu and S. Li (Eds.), International Symposium on Coal Combustion*, Springer, Singapore, 2019, P. 739–750.
36. **S. Wu, D. Che, Z. Wang, and X. Su**, NO_x emissions and nitrogen fate at high temperatures in staged combustion, *J. Energies*, 2020, Vol. 13, P. 3557.
37. **S. Li, S. Zhang, H. Zhou, and Z. Ren**, Analysis of air-staged combustion of NH₃/CH₄ mixture with low NO_x emission at gas turbine conditions in model combustors, *J. Fuel*, 2019, Vol. 237, P. 50–59.
38. **M. Kapusuz, A. Çakmak, and H. Özcan**, Application of oxygen enrichment and adiabatic humidification to suction air for reducing exhaust emissions in a gasoline engine, *J. Energy Sources Part A*, 2023, Vol. 45, No. 1, P. 194–211.
39. **D. Sun**, Experimental study on air humidification flue gas condensation waste heat recovery and NO_x purification system. MD Thesis, Architecture and Civil Engineering, Beijing University of Civil Engineering and Architecture, 2021. (In Chinese)
40. **H. Zhai**, Experimental study on direct expansion heat pump flue gas waste heat recovery and purification system. MD Thesis, Architecture and Civil Engineering, Beijing University of Civil Engineering and Architecture, 2020. (In Chinese)

41. **B. Sun, D. Wang, E. Duan, Y. Guo, W. Cao, and S. Zhang**, Study on NO_x formation characteristics under air staged combustion, *J. Journal of Power Engineering*, 2013, Vol. 33, P. 261–266. (In Chinese).
42. **B. Engin, U. Kayahan, and H. Atakül**, A comparative study on the air, the oxygen-enriched air and the oxy-fuel combustion of lignites in CFB, *J. Energy*, 2020, Vol. 196, P. 117021.
43. **J. Liu, X. Luo, S. Yao, Q. Li, and W. Wang**, Influence of flue gas recirculation on the performance of incinerator-waste heat boiler and NO_x emission in a 500 t/d waste-to-energy plant, *J. Waste Manage. (Oxford)*, 2020, Vol. 105, P. 450–456.
44. **F. Ren, L. Xiang, H. Chu, H. Jiang, and Y. Ya**, Modeling study of the impact of blending N₂, CO₂, and H₂O on characteristics of CH₄ laminar premixed combustion, *J. Energy Fuels*, 2019, Vol. 34, P. 1184–1192.
45. **S. Yonmo, and C. Gyungmin**, Effectiveness between swirl intensity and air staging on NO_x emissions and burnout characteristics in a pulverized coal fired furnace, *J. Fuel Process. Technol.*, 2015, Vol. 139, P. 15–24.
46. **P. Schmittel, B. Günther, B. Lenze, W. Leuckel, and H. Bockhorn**, Turbulent swirling flames: Experimental investigation of the flow field and formation of nitrogen oxide, *J. Proc. Combust. Inst.*, 2000, Vol. 28, P. 303–309.
47. **M. Ikeda, H. Makino, H. Morinaga, K. Higashiyama, and Y. Kozai**, Emission characteristics of NO_x and unburned carbon in fly ash during combustion of blends of bituminous/sub-bituminous coals, *J. Fuel*, 2003, Vol. 82, P. 1851–1857.